Eur. Phys. J. B **16**, 373–378 (2000)

THE EUROPEAN PHYSICAL JOURNAL B

EDP Sciences

Magnetic induction by coherent vortex motion

P. Odier[1], J.-F. Pinton[1,a], and S. Fauve[2]

[1] Laboratoire de Physique[b], École Normale Supérieure de Lyon, 46 allée d'Italie, 69007 Lyon, France
[2] Laboratoire de Physique Statistique[c], École Normale Supérieure, 24 rue Lhomond, 75005 Paris, France

Received 27 October 1999 and Received in final form 16 March 2000

Abstract. We investigate experimentally the advection of a magnetic field by a flow of conducting fluid, at moderate magnetic Reynolds numbers. More specifically, we study the influence of a large scale intense vortex on an externally applied field. We show that at large scales the magnetic field lines are distorted in a way that is consistent with a scenario of magnetic field expulsion by vorticity. Measurements at small scales show that the magnetic fluctuations are also quite sensitive to the large scale vortex motion.

PACS. 47.27.-i Turbulent flows, convection, and heat transfer – 47.65.+a Magnetohydrodynamics and electrohyrodynamics

1 Introduction

Magnetohydrodynamics in rotating flows is found in many instances of earth and planetary sciences [1]. For instance, a rotating gas cloud could not collapse without the existence of a magnetic field to remove its angular momentum. From a fluid mechanics point of view, the governing equation for the magnetic field [2]:

$$\frac{\partial \mathbf{B}}{\partial t} = \mathbf{curl}\,(\mathbf{u} \times \mathbf{B}) + \lambda \Delta \mathbf{B}, \tag{1}$$

is very similar to the equation for vorticity, albeit with different boundary conditions. On that basis, analogies have been proposed between vorticity and magnetic field [5,6]. In equation (1), we call $\mathbf{u}$ the velocity of a fluid with permittivity μ and conductivity σ; $\lambda \equiv 1/\mu\sigma$ is the magnetic diffusivity. The relative amplitude of the induction term to the dissipative one is given by the magnetic Reynolds number $R_m = UL/\lambda$. In liquid metals, λ is quite large compared to the fluid's kinematic viscosity ν. As a result R_m remains modest, even for quite large Reynolds number flows.

We consider here the topology and dynamics of $\mathbf{B}$ in the presence of a weak, externally applied field $\mathbf{B}_0$. The reason is that when $\mathbf{B}_0$ is small the motion of the fluid is not modified by the Lorentz force; the magnetic field does not react back on the flow field. The dynamics of $\mathbf{B}$ results from the combined effects of induction and diffusion (Joule dissipation). For an incompressible flow, the dynamical equation for $\mathbf{B}$ can be rewritten as that of a passive vector:

$$\frac{\partial \mathbf{B}}{\partial t} + (\mathbf{u} \cdot \boldsymbol{\nabla})\,\mathbf{B} = (\mathbf{B} \cdot \boldsymbol{\nabla})\,\mathbf{u} + \lambda \Delta \mathbf{B}. \tag{2}$$

Save for the dissipative term, this is the equation of motion of a material line of fluid, which is both advected and stretched by the flow. The presence of the stretching term is of uttermost importance, since at high R_m, it may overcome Joule dissipation and generate a large scale magnetic field by amplification of weak initial disturbances. This is known as the dynamo effect [3]. Magnetic field dynamics is also often considered as being at an intermediate complexity level in turbulence, between the passive vector problem and the full vorticity dynamics.

In this work we address experimentally the relationship between vorticity and magnetic field. Specifically, we study how a strong vortex acts on an externally applied field, initially uniform. The velocity gradients generate an induced component which modifies the magnetic field topology and fluctuations. The experimental flow is produced in the gap between coaxial disks and the conducting fluid is gallium. The results of measurements in the turbulent, counter-rotating case have been reported in [4]. We concentrate here on the corotating case where the flow is dominated by the presence of a strong large scale vortex.

2 Experimental set-up and flow characteristics

Our experimental setup is schematically shown in Figure 1. The flow belongs to the so-called von Kármán geometry [9]. Two 11 kW ac-motors are used to drive rugose disks (they bear an etched pattern in the form of squares 1 mm thick) of radius $R = 9$ cm at a constant rotation rate

[a] e-mail: pinton@ens-lyon.fr
[b] CNRS, UMR 5672
[c] CNRS, UMR 8550

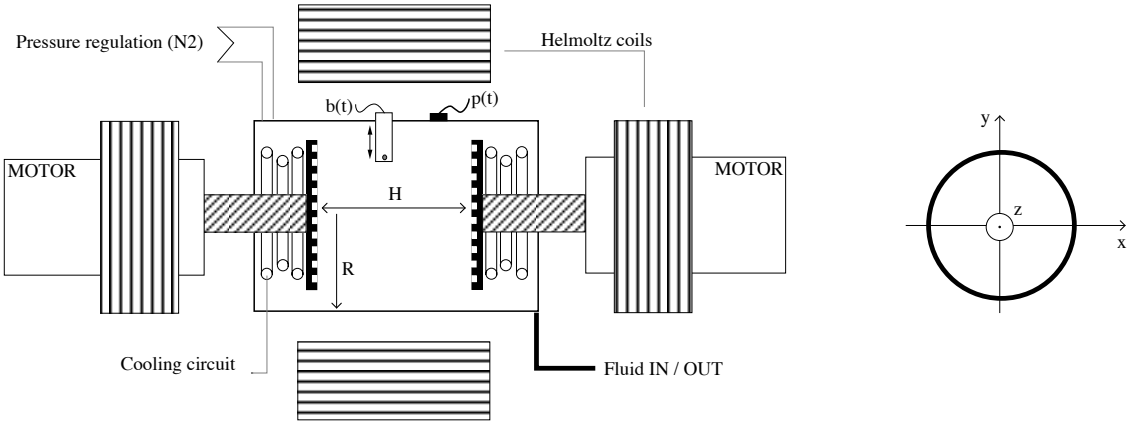

Fig. 1. Experimental setup and orientation conventions: the z-axis is parallel to the rotation axis of the motors and the x-axis is parallel to the axis of the transverse Helmoltz coils.

Table 1. Main physical properties of liquid gallium.

Heat capacity [$\mathrm{J\,kg^{-1}\,K^{-1}}$]	$C = 3.847 \times 10^2$
Density	$\rho = 6.09$
Viscosity [$\mathrm{m^2\,s^{-1}}$]	$\eta = 3 \times 10^{-7}$
Thermal conductivity [$\mathrm{W\,m^{-1}\,K^{-1}}$]	$k = 29.8$
Electrical conductivity [$\Omega^{-1}\ \mathrm{m^{-1}}$]	$\sigma = 3.7 \times 10^6$

using a tachymetry feed-back loop, with a stability better than 0.1%. The disks are corotating with rotation rates which can be adjusted between 10 and 50 Hz (3 000 rpm). They are set at a distance $H = 10$ cm apart. The enclosing cylindrical vessel, with inner radius $R = 10$ cm and inner height 20 cm, has a volume of 5.5 liters. It is filled with liquid gallium chosen for its high electrical conductivity; its main physical properties are recalled in Table 1. The flow is cooled using controled water circulators.

We perform magnetic measurements in the following manner: two pairs of Helmholtz coils are set to produce an external field B_0 up to 20 gauss, either parallel or perpendicular to the rotation axis, *i.e.* aligned with the $z-$ or $x-$axis (see Fig. 1). The field is then recorded inside the vessel using directional Hall probes with a Bell 9905 gaussmeter; the spatial resolution is 3 mm, with a frequency range of 50 kHz in AC mode or 400 Hz in DC mode. The resolution in time of the measurement is in fact limited by the spatial extend of the probe: with typical velocities of the order of 12 m/s (the disks rim speed) and a probe width of 3 mm, one expects a cut-off at about 4 kHz. Pressure measurements are made with a 5 mm PCBH112A21 piezoelectric transducer, mounted flush with the lateral wall, in the mid-plane between the disks. It is acceleration-compensated and has a low frequency cut-off at -3 dB equal to 50 mHz; its rise-time is 1 ms. Data are digitized using a 16 bits acquisition card in a PC computer.

The integral kinematic and magnetic Reynolds numbers of the flow are defined as: $Re = 2\pi R^2 \Omega/\nu$ and $Rm = 2\pi\mu_0\sigma R^2\Omega$. In typical runs $Re \sim 10^6$ and $Rm \sim 10$. In the case of the confined corotating von Kármán flow, our previous studies using water as a working fluid have shown

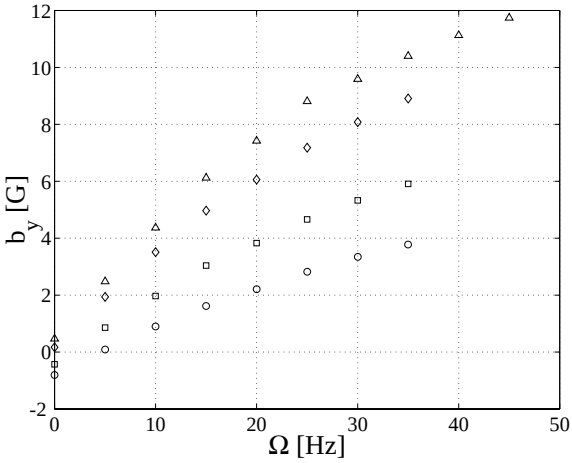

Fig. 2. Evolution of vertical induced component b_y with the discs rotation rates, for $B_{0x} = 17$ G, for $y = 5$ cm ($\triangle$), 7 cm ($\diamond$), 9 cm ($\square$) and inside the steel container ($\circ$).

that when the disks rotation rates are equal rates a strong axial vortex is formed [10].

3 Results

3.1 Large scale topology

Consider the case of an externally applied field $\mathbf{B}_0$, uniform and parallel to the x-direction. We observe that the swirling motion creates a component in the y-direction, whose magnitude is proportional both to the intensity of the applied field and to the rotation rate of the vortex. We have checked that the induced component b_y is proportional to the applied field B_0. Figure 2 shows its variation with Ω, measured at different depths inside the flow. One observes a steady increase of b_y with Ω. In the limit of small magnetic Reynolds numbers, this can be understood as follows. Since the magnetic diffusivity is orders of magnitude larger than the kinematic viscosity, the induced field $\mathbf{b}$ adiabatically follows $\mathbf{u}$. In this "quasistatic"

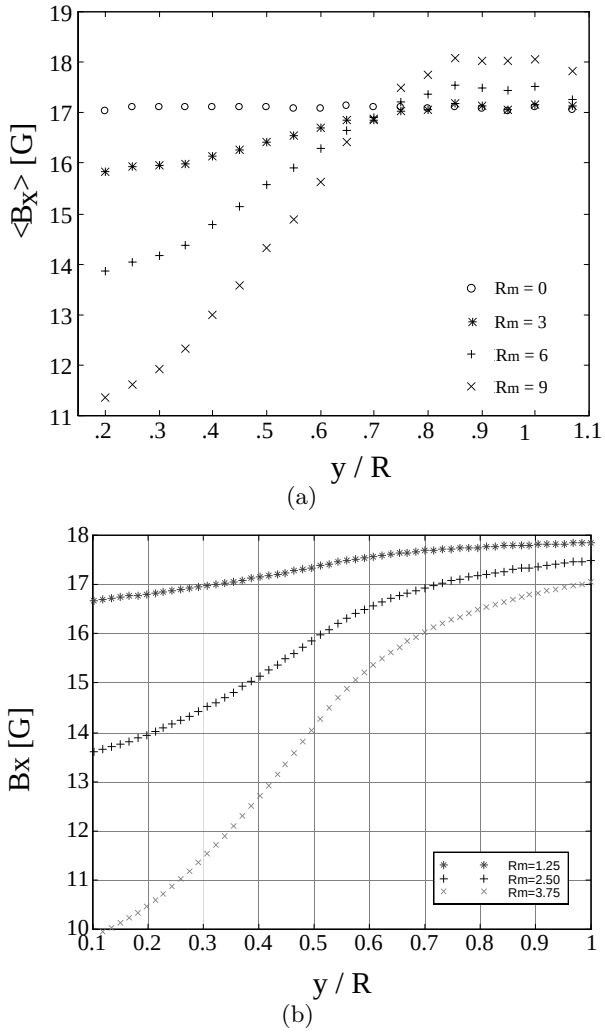

Fig. 3. (a) Profile of total magnetic field component B_x parallel to the applied field (B_{0x}), for $Rm = 0(\circ)$, $Rm = 3(*)$, $Rm = 6(+)$, $Rm = 9(\times)$. (b) Corresponding simulated profiles, in the case of a 2D vortex in solid body rotation.

approximation [12,13], equation (2) yields to leading order:

$$\lambda \Delta \mathbf{b} \approx -(\mathbf{B}_0 \cdot \boldsymbol{\nabla})\mathbf{u}, \tag{3}$$

that is an induced field proportional to Rm. In the geometry discussed here, one has $\lambda \Delta b_y \approx -B_0 \partial_x u_y$, or if we assume an axisymetric velocity field, $\lambda \Delta b_y \approx -B_0 \omega_z$, where $\boldsymbol{\omega}$ is the vorticity. From that relationship follows the linearity of b_y with both the applied field and the discs rotation rate (the vorticity is directly proportional to Ω). It also shows the particular role played by the vorticity in the generation of the induced magnetic field. However it is assumed in equation (3) that the induced field is much smaller than the applied one. It is obviously not the case here; Figure 2 shows that the induced component can be of the order of magnitude of the applied field! In addition, we observe that the variation $b_y(\Omega)$ is not linear, in particular in the vicinity of the vortex core.

One can also view the creation of induced field as being the result of the circulation of induced currents. If one 'un-

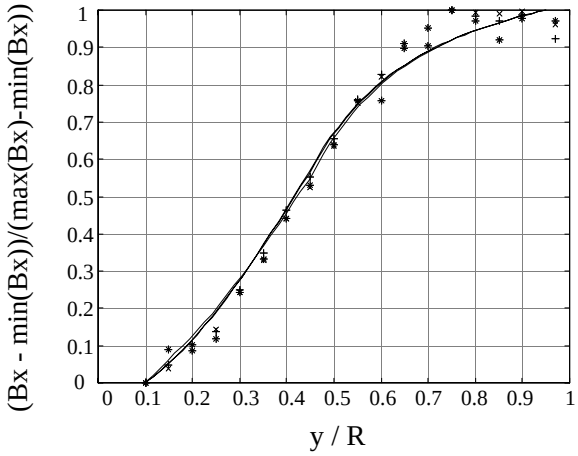

Fig. 4. Measured and computed B_x profiles, in reduced units.

curls' equation (1) in a stationary context, one obtains the induced current, whose main contribution is $\mathbf{j} \sim \sigma(\mathbf{u} \times \mathbf{B}_0)$. That is, the large scale rotation produces mainly a current aligned with the axis of rotation (z-axis) that circulates in one direction in one half of the cylinder and in the other in the other half. These currents generate a transverse magnetic field, parallel to the y-axis. Note that if the direction of $\mathbf{B}_0$ is reversed, so is $\mathbf{j}$ and hence b_y: the phenomenon is actually a consequence of the advection of the magnetic field lines by the fluid motion.

The influence of plane differential rotation on an initialy uniformed field has been investigated analytically and numerically by several authors [14,7,6]. They have shown that at the onset of motion the magnetic field lines are distorted and stretched; the magnetic field inside the vortex increases until diffusion acts and leads to a steady states where the field is actually *reduced* inside the vortex. This effect is known as the expulsion of magnetic field from eddies. The duration τ of the transient regime is of the order of the vortex turnover time, too fast to be resolved with precision in our experiment[1]. However we can test the predictions on the steady state. Figure 3a shows measurements of the magnetic field component parallel to the applied field for several values of the discs rotation rate. The profile is obtained by displacement of the Hall probe along the y-axis. We observe that inside the vortex core, B_x decreases as Rm increases. For the maximum Reynolds number of the experiment, it is reduced to 60% of its original value on the axis. The measurements can be compared to analytical solutions in the case of a 2D vortex in solid body rotation – *cf.* Moffatt [6], pp. 54-58. They are shown in Figure 3b, where we have chosen a vortex core size equal to 5 cm. One can see that there is a good agreement for the reduction of the field on the axis, for a given value of the vortex rotation rate and core size. Note that in order to compare the magnetic Reynolds numbers in the experiment and in the computation, one must recalculate the experimental Rm based on the vortex core

[1] There is also a debate on its dependence with Rm: Parker [14] and Weiss [7] obtain $\tau \sim O(Rm^{1/3})$, while Moffatt derives $\tau \sim O(Rm^{1/2})$, a difference that would be hard to settle in a low Rm experiment such as ours.

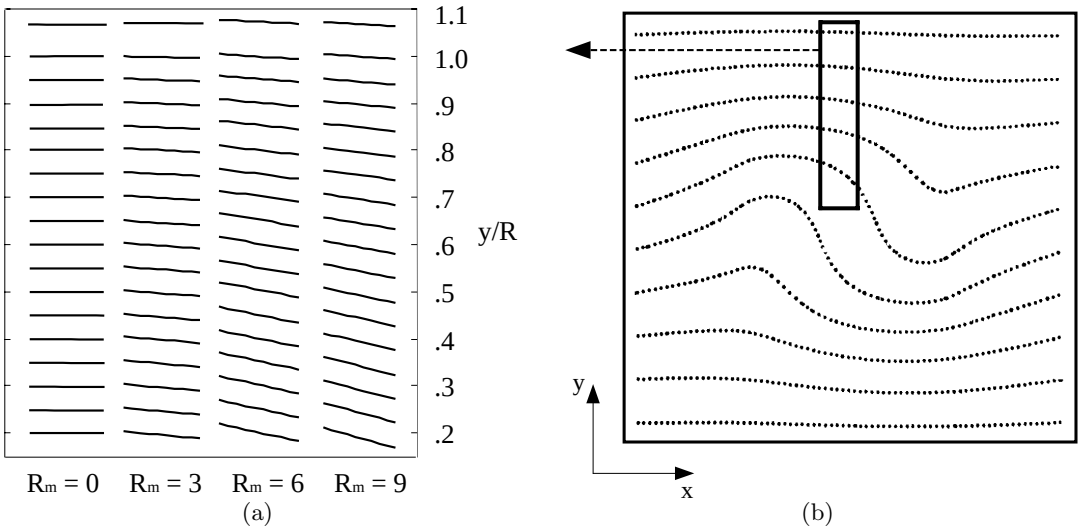

Fig. 5. (a) Orientation of field lines, calculated from B_x and B_y measurements; (b) Computed field lines, from [7] Figure 10c, at $Rm = 20$. The measurement in (a) corresponds to the highlighted slab in the calculated profile in (b).

size and turnover time; one obtains $Rm' = 1.1, 2.2, 3.3$. For a complete description of the details of the profiles, one would have to know the actual vorticity distribution in the experiment. In fact, the difference with the computed profile provides information about the flow vorticity distribution. Figure 4 shows the magnetic field profiles in reduced units $(B - B_{\min})/(B_{\max} - B_{\min})$. We first observe that at all Rm the B_x-profiles are self similar as revealed by the collapse of the measurement in reduced units. From an hydrodynamics point of view, it indicates that as the rotation rate of the disks increase, the magnitude of vorticity increases but its distribution remains unchanged, in particular the core size. This results confirms independent studies [15,11] which have shown that the vorticity profile in this flow is set by the geometry (in particular the shape of the driving disks) and does not vary with the imposed rotation rate. Secondly, we note that there is a good agreement between the experimental profile and the calculated one, showing that a vortex core in solid body rotation is an adequate model for the vorticity distribution of this flow. The measurements in the x and y directions can be put together to obtain the distortion of the initial field lines. This is drawn in Figure 5, again with the model flow picture for comparison; the experimental measurements shown in Figure 5a corresponds to a thin slab in a full two-dimensional profile such as the calculated one shown in Figure 5b. We observe the predicted magnetic lines twisted by vorticity.

If one further assumes that the flow is bidimensional near the measurement zone we can evaluate the local magnetic energy as $E_B \sim \left(B_x^2 + B_y^2\right)/2\mu_0$ (we have checked that B_z remains small: $B_z < 0.2$ G, for $B_0 = 17$ G). The result is given in Figure 6: we observe a decrease inside the vortex core region, but a significant increase outside. It is again linked to the distortion of the field lines by the swirling fluid motion: initially equally spaced field lines are expelled from the vortex core and brought together outside, as illustrated in Figure 5b.

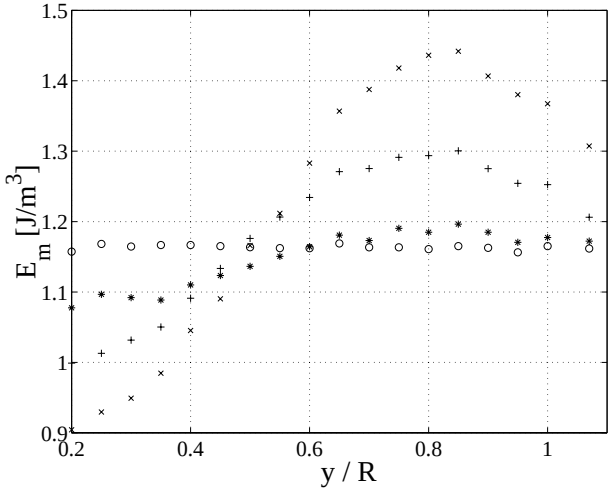

Fig. 6. Profile of magnetic energy, $E_B \sim B_x^2 + B_y^2$, for $Rm = 0(\circ)$, $Rm = 3(*)$, $Rm = 6(+)$, $Rm = 9(\times)$.

3.2 Fluctuations

We now consider the fluctuations of the magnetic field. A first remark is that the large scales fluctuations in the magnetic field follow the evolution of the flow. This is shown – Figure 7 – using simultaneous measurements of magnetic field and pressure fluctuations at the flow wall [16]. As observed in [10], the rotation of the disks generate a vortex at the same rotation rate Ω which can be observed simultaneously in the pressure and magnetic measurements (Figs. 7a and 7b). Such frequency lines are related to the vortex motion since they are not observed when the disks are counter-rotating at the same rate Ω. In addition, we note the strong coherence between the pressure and magnetic variations – Figure 7c – as further evidence of correlation between vorticity and dynamics of magnetic induction.

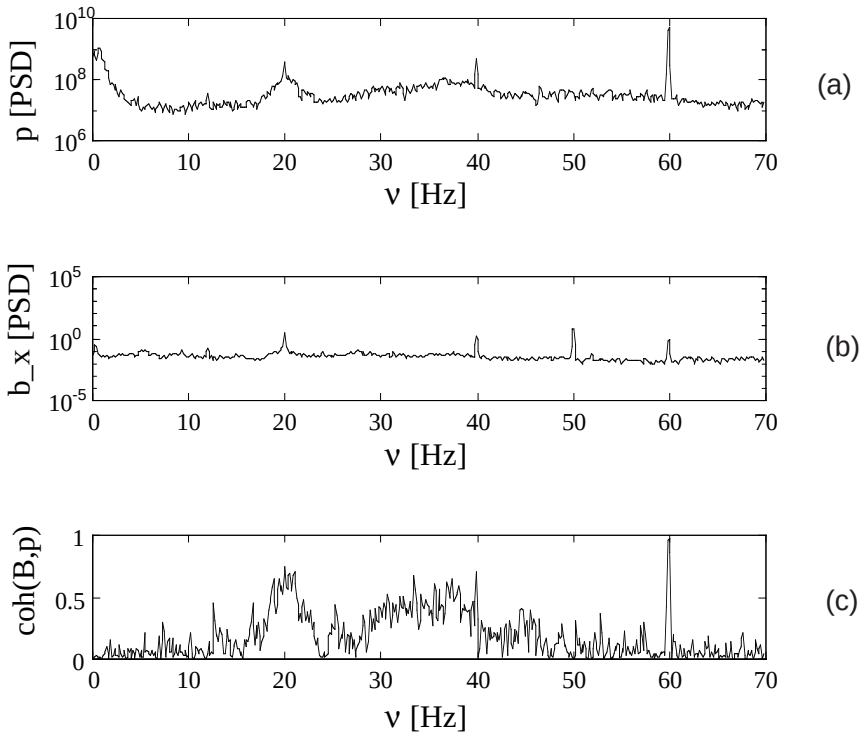

Fig. 7. Corotating flow at $\Omega = 20$ Hz. (a) Power spectral density of pressure fluctuations at the flow wall. (b) Power spectral density of magnetic field measured 1 cm inside the flow. (c) Coherence of magnetic and pressure signals.

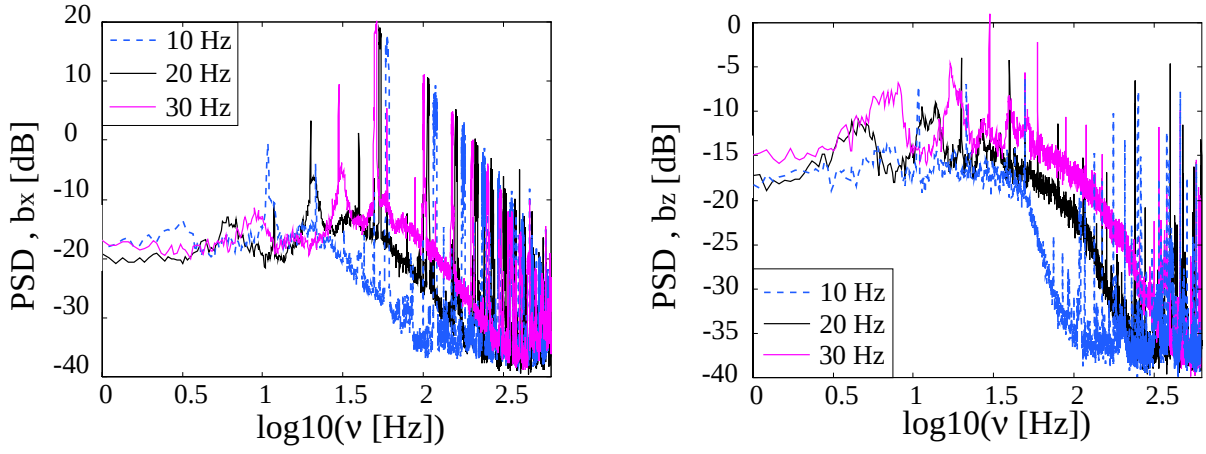

Fig. 8. Power spectra of magnetic fluctuations. The probe is located in the mid plane between the disks and 1 cm inside the vessel. The applied is in the x direction. The measured component is in the x direction in (a) and along the z direction in (b).

Another observation concerns the turbulent fluctuations. They are present, because as already mentioned the flow is quite turbulent. Due to the small kinematic viscosity of gallium, the integral Reynolds number $Re = 2\pi R^2 \Omega/\eta$ is of the order of 10^6 in this flow. Several studies using air or water as working fluids have shown that when the disks are counter-rotating, a very intense, almost homogeneous turbulence is generated [17]. As a results, and in agreement with Kolmogorov's scaling, our measurements in the counter-rotating case have shown that the magnetic spectra display an inertial range where $B^2(\nu) \propto \nu^{-11/3}$ (here, ν is the time frequency) [4]. In the corotating case, turbulent fluctuations are superimposed to the strong axial vorticity.

Figure 8 shows the spectra of magnetic fluctuations, for an applied field in the x-direction, the measurements being made in the same x direction (8a) or along the axis z of rotation (8b). Peaks corresponding to the rotation rate of the disks are observed at low frequencies. At higher frequencies, one observes a strong anisotropy: the b_x

component follows a decrease with a $\nu^{-11/3}$ behaviour as in homogeneous turbulence, but the b_z component has a much steeper fall-off, that does not follow a power law. In addition in this case, energetic fluctuations exist at much higher frequencies: in Figure 8, b_z has a roughly constant energy content up to 200 Hz (at $\Omega = 30$ Hz, for example) whereas at that frequency the fluctuations in b_x are one order of magnitude smaller. The anisotropy of the large scale flow is thus observed on the velocity gradients (which produce the magnetic induction) at all scales. This is consistent with direct local measurements of the velocity field in similar experiments in air where we have shown that the presence of the vortex influences the turbulent velocity fluctuations across the entire range of scales of turbulent eddies [11].

4 Concluding remarks

The measurements reported in the first section show that, from a stationary point of view, there is a strong (anti)correlation between B and ω: regions of high vorticity tend to expel a transverse magnetic field. Our measurements are in agreement with the scenarios and calculations proposed by Parker, Weiss and Moffat [14,7,6]. This correlation is also a dynamical one and we observe that the presence of vorticy introduces a strong anisotropy in the fluctuations of the magnetic field at all scales. It may be of importance in MHD turbulence and deserves further investigations.

This work is supported by grants from Centre National de la Recherche Scientifique. We thank Rhône-Poulenc for making the gallium available to us. The authors are greatful to Marc Moulin for continuous technical assistance and development on the gallium setup.

References

1. W.M. Elsasser, Am. J. Phys. **23**, 590 (1955).
2. P.H. Roberts, *An introduction to magnetohydrodynamics* (Longmans, 1967).
3. The dynamo effect is discussed in several textbooks, such as [2]. Kinematic simulations in flow geometries linked to our experimental setup are reported in N.L. Dudley, R.W. James, Proc. Roy. Soc. Lond. A **425**, 407 (1989).
4. P. Odier, J.-F. Pinton, S. Fauve, Phys. Rev. E **56**, 7397 (1998).
5. G.K. Batchelor, ProC. Roy. Soc. A **201**, 405 (1950).
6. H.K. Moffatt, *Magnetic field generation in electrically conducting fluids* (Cambridge U.P., 1978).
7. N.O. Weiss, Proc. Roy. Soc. A **293**, 310 (1966).
8. O. Cadot, S. Douady, Y. Couder, Phys. Fluids **7**, 630 (1995); B. Dernoncourt, J.-F. Pinton, S. Fauve, Physica D **1910**, 1 (1998).
9. P.J. Zandberg, D. Dijkstra, Ann. Rev. Fluid Mech. **19**, 465 (1987).
10. J.-F. Pinton, F. Chillà, N. Mordant, Eur. J. Mech. B Fluids **17**, 535 (1998).
11. C. Simand, F. Chillà, J.-F. Pinton, Europhys. Lett. **49**, 336 (1999).
12. G.S. Golitsyn, Sov. Phys. Dokl. **5**, 536-539 (1960).
13. H.K. Moffatt, J. Fluid Mech. **11**, 625 (1961).
14. E.N. Parker, Astrophys. J. **138**, 552-575 (1963).
15. B. Andreotti, *Action et réaction entre étirement et rotation, du laminaire au turbulent*, Ph.D. thesis, École Normale Supérieure, 1999.
16. Pressure fluctuations at the flow wall are related to the dynamics of the flow, S. Fauve, C. Laroche, B. Castaing, J. Phys. II France **3**, 271 (1993); N. Mordant, F. Chillà, J.-F. Pinton, J. Phys. II France **7**, 1 (1997).
17. J.-F. Pinton, R. Labbé, J. Phys. II France **4**, 1461 (1994); J. Maurer, P. Tabeling, G. Zocchi, Europhys. Lett. **26**, 31 (1994).